HHS Public Access

Author manuscript

Curr Biol. Author manuscript; available in PMC 2021 January 20.

Published in final edited form as:

Curr Biol. 2020 January 20; 30(2): 359–366.e3. doi:10.1016/j.cub.2019.11.085.

Steroid Hormone Entry into the Brain Requires a Membrane Transporter in *Drosophila*

Naoki Okamoto, **Naoki Yamanaka***

Department of Entomology, Institute for Integrative Genome Biology, University of California, Riverside, 900 University Ave., Riverside, CA 92521, USA

SUMMARY

Steroid hormones control various aspects of brain development and behavior in metazoans, but how they enter the central nervous system (CNS) through the blood-brain barrier (BBB) remains poorly understood. It is generally believed that steroid hormones freely diffuse through the plasma membrane of the BBB cells to reach the brain [1], because of the predominant “simple diffusion” model of steroid hormone transport across cell membranes. Recently, however, we challenged the simple diffusion model by showing that a *Drosophila* organic anion transporting polypeptide (OATP), which we named Ecdysone Importer (EcI), is required for cellular uptake of the primary insect steroid hormone ecdysone [2]. As ecdysone is first secreted into the hemolymph before reaching the CNS [3], our finding raised a question of how ecdysone enters the CNS through the BBB to exert its diverse role in *Drosophila* brain development. Here we demonstrate in the *Drosophila* BBB that EcI is indispensable for ecdysone entry into the CNS to facilitate brain development. EcI is highly expressed in surface glial cells that form the BBB, and *EcI* knockdown in the BBB suppresses ecdysone signaling within the CNS and blocks ecdysone-mediated neuronal events during development. In an *ex vivo* culture system, the CNS requires EcI in the BBB to incorporate ecdysone from the culture medium. Our results suggest a transporter-mediated mechanism of steroid hormone entry into the CNS, which may provide important implications in controlling brain development and behavior by regulating steroid hormone permeability across the BBB.

eTOC Blurb

Steroid hormones are thought to freely diffuse across the blood-brain barrier (BBB) due to the predominant “simple diffusion” model of their transport across cell membranes. Okamoto and Yamanaka now provide evidence that the insect steroid hormone ecdysone requires an SLCO superfamily transporter EcI in the BBB to enter the brain in *Drosophila.*

*Correspondence and Lead Contact: naoki.yamanaka@ucr.edu.

AUTHOR CONTRIBUTIONS

Conceptualization, N.O. and N.Y.; Methodology, N.O. and N.Y.; Investigation, N.O.; Writing, Review & Editing, N.O. and N.Y.; Supervision, N.Y.; Funding Acquisition, N.O. and N.Y.

DECLARATION OF INTERESTS

The authors declare no competing interests.

Graphical Abstract

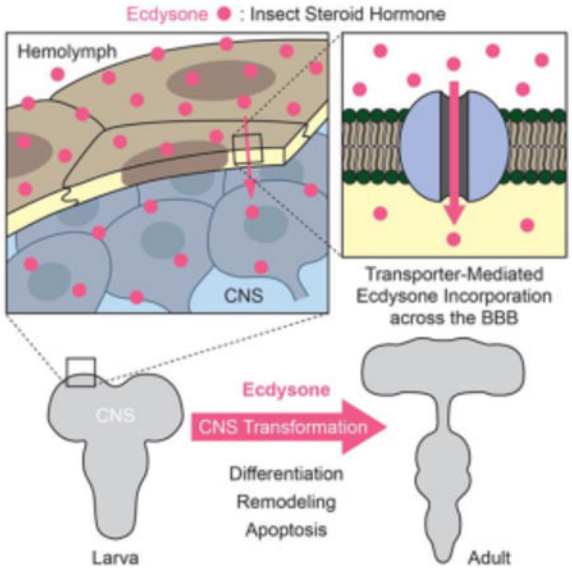

RESULTS

EcI in the BBB Is Required for Ecdysone-Mediated Innate Behaviors

We raised antibodies against EcI and detected a strong EcI immunoreactivity around the CNS, suggesting predominant *EcI* expression in surface glial cells (Figure 1A). In *Drosophila,* surface glial cells form septate junctions and cover the entire CNS [4–6], thus manifesting the property of the BBB that has structural and functional similarities to the mammalian endothelial cells that form tight junctions around the blood vessels [7–10]. The corresponding signal was abolished by RNAi-mediated knockdown of *EcI* in the BBB by using *9–137-Gal4* (Figure 1B), which drives specific and strong expression in the BBB [11] (Figures S1A and S1B). This demonstrates that EcI is indeed highly expressed in the BBB as reported previously [10, 11], although its immunoreactivity was also detected in multiple populations of cells within the CNS, such as neuroepithelial cells (Figure 1B). We also analyzed a GFP enhancer trap line of *EcI (Mi{MIC}Oatp74D*^{MI05878} or *EcI*^{MI05878}*)* [12] and detected a prominent GFP signal surrounding the CNS, further confirming its high BBB expression (Figures S1C and S1D).

To analyze the function of EcI in the BBB, we conducted BBB-specific knockdown of *EcI* or *EcR* by using *9–137-Gal4.* Other known BBB-Gal4 lines tested *(Moody-Gal4* [5], *NP2276-Gal4,* and *NP6293-Gal4* [13]) drive prominent *Gal4* expression in other tissues during development (Figure S1A). At the onset of metamorphosis, late third instar (L3) larvae reared in fly culture vials typically crawl out of the food and exhibit wandering behavior before pupariation. Although control or *EcR* RNAi larvae showed normal wandering behavior and pupariated on the vial wall, *EcI* RNAi larvae failed to exit the food and pupariated in/on the food (Figures 1C and D). Previous studies have suggested that insect wandering behavior is induced by ecdysone signaling in brain neurons [14–16]. Furthermore, the majority of *EcI* RNAi but not *EcR* RNAi prepupae failed to perform head

eversion during pupal ecdysis and died at the prepupal stage (Figure S2), potentially due to the lack of ecdysone-induced ecdysis triggering hormone receptor expression in the CNS [17]. These results suggest that EcI in the BBB is required for circulating ecdysone to access the neural substrates within the CNS that are responsible for ecdysone-mediated innate behaviors. Interestingly, when *EcR* expression was suppressed in the BBB, most animals failed to eclose and died as pharate adults (Figure S2), suggesting the importance of ecdysone signaling within the BBB itself to complete metamorphosis.

EcI in the BBB Is Required for the Activation of Ecdysone Signaling in the CNS

We next examined the ecdysone signaling activity in the CNS using the ecdysone response element (EcRE)-driven *LacZ* (*EcRE-LacZ)* reporter [18], while knocking down *EcR* or *EcI* specifically in the BBB. When hemolymph ecdysone is at its basal level (early and mid L3 stages; 0 hour after L3 ecdysis [0 hAL3E] and 24 hAL3E), *EcRE-LacZ* expression levels are equally low in the CNS of all animals (Figures 2A–2C). At the white prepupal stage (0 hour after puparium formation [0 hAPF]), when ecdysone titer is at its peak, the *EcRE-LacZ* expression is significantly increased in the CNS in control and *EcR* RNAi animals (Figures 2A–2C). High *EcRE-LacZ* expression was observed in two neuroepithelia known as the inner and outer proliferation centers, BBB, and specific populations of cells within the control CNS (Figures 2A and 2B). Importantly, in *EcR* RNAi animals, *EcRE-LacZ* expression was only reduced in the BBB but not within the CNS at 0 hAPF (Figure 2B), indicating that ecdysone signaling within the BBB itself is not necessary for the activation of ecdysone signaling in the other populations of cells in the CNS. In clear contrast, in *EcI* RNAi animals, *EcRE-LacZ* expression was significantly reduced not only in the BBB but in the entire CNS at 0 hAPF (Figures 2A–2C). Taken together, these results demonstrate that EcI but not EcR in the BBB is required for ecdysone signaling within the CNS, suggesting that EcI is rather required for transcellular transport of circulating ecdysone across the BBB into the CNS.

EcI in the BBB Regulates Ecdysone-Mediated Neuronal Events during Development

In mammals, steroid hormones are known to affect multiple aspects of brain development [19–21]. Similarly, in *Drosophila,* ecdysone controls neuronal remodeling, differentiation, and programmed cell death during metamorphosis to transform the CNS to adapt to adult-specific physiology and behaviors [22–28]. We therefore analyzed the morphology of the CNS during development in the BBB-specific *EcR* or *EcI* RNAi animals (Figure 3A). The CNS from both control and *EcR* RNAi animals showed dramatic morphological changes after puparium formation, although *EcR* RNAi animals showed a slight defect in the separation of the subesophageal and thoracic ganglia (Figure 3A, arrow). Importantly, however, we found that BBB-specific *EcI* knockdown severely impaired the CNS transformation, and the CNS retained its larval morphology even at 24 hAPF (Figure 3A).

We next analyzed ecdysone-mediated neuronal events such as differentiation, remodeling, and programmed cell death during development [25–27]. Prior to metamorphosis, a pulse of ecdysone during the mid to late larval stage triggers the differentiation of neuroepithelial cells into medulla neuroblasts [29]. In the CNS of the BBB-specific *EcI* RNAi animals, the region of medulla neuroblasts decreased dramatically as compared to the CNS from control

and *EcR* RNAi animals (Figures 3B, S3A, and S3B). During metamorphosis, a high level of ecdysone induces remodeling of mushroom body neurons [26, 27, 31, 32]. In both control and *EcR* RNAi animals, the larval-specific γ lobe of the mushroom body was completely pruned and α/β neurons extend their axons at 24 hAPF, whereas this remodeling was blocked and γ lobe was still intact in *EcI*RNAi animals (Figure 3C). Moreover, it is known that a subset of larval corazonin-producing neurons in the ventral nerve cord (vCrz neurons) undergo ecdysone-induced apoptosis and are eliminated during metamorphosis, whereas three pairs of corazonin-producing neurons in the dorso-lateral region (dlCrz neurons) persist into the adult brain [33]. Although vCrz neurons were eliminated in control and *EcR* RNAi animals at 24 hAPF, both dlCrz and vCrz neurons remained intact in the CNS of *EcI* RNAi animals (Figures 3D and S3C). Altogether, these results demonstrate that EcI in the BBB is required for ecdysone-mediated neuronal events in the CNS during development.

EcI in the BBB Is Required for the Incorporation of Circulating Ecdysone into the CNS

Lastly, we examined the effect of the active form of ecdysone, 20-hydroxyecdysone (20E), on *EcRE-LacZ* expression by using an *ex vivo* CNS culture system. We specifically knocked down *EcI* in the BBB, and *ex vivo* culture of the CNS from the mid L3 larval stage (24 hAL3E) was conducted with or without 20E. 20E concentrations were determined based on the ecdysteroid concentration in the hemolymph during mid L3 to white prepupal stage ($1 \times 10^{-8} – 3 \times 10^{-7}$ M) [2, 34]. Knockdown of *EcI* in the BBB significantly reduced dose-dependent induction of *EcRE-LacZ* expression by 20E in the cultured CNS (Figures 4A and 4B). Notably, dynamic morphological changes induced by high concentrations of 20E (3×10^{-7} and 1×10^{-6} M) in the control CNS were completely suppressed in the *EcI* RNAi samples (Figure 4A). The morphological changes of the cultured CNS can be explained by ecdysone-dependent neurogenesis during optic lobe development [29, 35]. Indeed, stimulation of 5-ethynyl-2’-deoxyuridine (EdU) incorporation by 20E was observed in the cultured CNS, especially around the optic lobe region (Figure S4). In contrast, knockdown of *EcI* in the BBB significantly reduced EdU incorporation induced by 20E (Figure S4). Importantly, knockdown of *EcI* in the BBB does not affect *EcRE-LacZ* activity induced by a non-steroidal ecdysone agonist chromafenozide [36], which does not require EcI to traverse cell membranes [2] (Figures 4A and 4B). Taken together, these results demonstrate that EcI is required in the BBB for ecdysone incorporation from circulating hemolymph into the CNS (Figure 4C).

DISCUSSION

The CNS is physically separated from circulation by the BBB, which maintains proper ionic conditions, metabolic homeostasis, and hormonal state within the CNS to ensure normal neuronal development and functions [37–39]. However, because of the predominant “simple diffusion” model, it has long been assumed that the regulation of steroid hormone transport across the BBB only happens through active elimination by efflux transporters [40, 41]. In the present study, we challenged this view by demonstrating that Ecl, a membrane transporter required for cellular uptake of the insect steroid hormone ecdysone, is indispensable for transcellular transport of ecdysone across the BBB during *Drosophila* brain development.

Transporter-Mediated Ecdysone Incorporation into the CNS

For molecules that cannot take the paracellular route or freely diffuse through the BBB, there are two major mechanisms through which they are incorporated into the CNS [42]. One is transcytosis, which involves endocytosis of molecules from circulation into the BBB cells, intracellular vesicular trafficking, and exocytosis into the brain parenchyma [43]. The other mechanism is carrier-mediated transport, where molecules are first incorporated from circulation into the cytoplasm of the BBB cells by carrier proteins such as membrane transporters, after which they are exported into the brain [44]. Our results indicate that ecdysone is incorporated into the *Drosophila* CNS through the latter mechanism. Although the level of ecdysone signaling in the CNS generally correlates well with the hemolymph levels of ecdysone during normal development [45] (Figure 2), it is conceivable that BBB permeability becomes a limiting factor for ecdysone signaling within the CNS under abnormal conditions. Tools developed in our current study should facilitate future investigation of such possibilities.

Regulation of Lipophilic Hormone Permeability across the BBB by Organic Anion Transporting Polypeptides

Although the simple diffusion model has long been predominant for all steroid hormones, membrane transporters have been identified and their pathophysiological roles have been described for thyroid hormones, another group of lipophilic hormones in mammals [46–50]. Interestingly, among several membrane transporters with thyroid hormone transporting capacity are OATPs [51], the family of solute carrier transporters that Ecl belongs to [2]. Moreover, it has been shown that these thyroid hormone transporters, including OATPs, are expressed in the BBB and play critical roles in thyroid hormone incorporation into the brain [52–54], lack of which leads to neurological disorders [55–58]. It would therefore be important to investigate functions of OATPs in controlling permeability of lipophilic hormones, including steroid hormones, across the BBB in mammals. Considering that multiple inhibitors of mammalian OATPs have already been characterized [59], elucidation of hormone-transporting functions of OATPs across the BBB may lead to novel research techniques as well as clinical tools to manipulate lipophilic hormone signaling within the brain.

STAR⋆METHODS

LEAD CONTACT AND MATERIALS AVAILABILITY

Further information and requests for resources and reagents should be directed to and will be fulfilled by the Lead Contact, Naoki Yamanaka (naoki.yamanaka@ucr.edu).

Guinea pig anti-EcI antibodies generated by this study are available upon request.

EXPERIMENTAL MODEL AND SUBJECT DETAILS

Flies—All flies were raised at 25°C under 12 hours/12 hours light/dark cycle. The animals were reared on standard fly food containing 6 g *Drosophila* agar type II (Genesee Scientific, #66–103), 100 g D-(+)-glucose (SIGMA, #G8270–25KG), 50 g inactive dry yeast (Genesee Scientific, #62–106), 70 g yellow corn meal (Genesee Scientific, #62–101), 6 ml propionic

acid (SIGMA, #402907–500ML), and 10 ml Tegosept (Genesee Scientific, #20–258) in 1,025 ml of water. Flies used are as follows: w^{1118} (#5905; the control strain), *Mi{MIC}Oatp74D*^{MI05878} (#42353), *EcRE-LacZ* (#4516 and #4517), *UAS-EcR RNAi* (#9327), and *UAS-mCD8-GFP* (#5130) were obtained from the Bloomington *Drosophila* Stock Center (BDSC); *UAS-dicer2* (#60008 and #60009) was obtained from the Vienna *Drosophila* Resource Center (VDRC); *UAS-EcI (Oatp74D) RNAi* (#7571R-1) was obtained from the National Institute of Genetics Fly Stock Center; *NP2276-Gal4* (#112853) and *NP6293-Gal4* (#105188) were obtained from the Kyoto Stock Center (Department of *Drosophila* Genomics and Genetic Resources, Kyoto Institute of Technology). *9–137-Gal4* and *Moody-Gal4* were obtained from Ulrike Heberlein (Janelia Research Campus) and Ulrike Gaul (Ludwig-Maximilians-Universität München), respectively.

METHOD DETAILS

Immunostaining—The CNS was dissected in 1X phosphate-buffered saline (PBS) (Fisher BioReagents), fixed with 4% paraformaldehyde (PFA) (Electron Microscopy Sciences) in PBS (4% PFA/BBS) containing 0.1% TritonX-100 for 20 min at room temperature (RT), and washed multiple times with PBS containing 0.1% Triton X-100 (0.1% PBST). The tissues were blocked with 5% normal goat serum (NGS) (Sigma-Aldrich) in PBST for at least 1 hour at RT, incubated overnight at 4°C with the primary antibody mix in PBST containing 5% NGS, washed multiple times with PBST, incubated for 2 hours at RT with the secondary antibody mix in PBST containing 5% NGS, and washed multiple times again with PBST. When needed, DNA was stained with Hoechst 33342 (Thermo Fisher Scientific) at 1:2000 for 30 min at RT. After washing, tissues were mounted in Vectashield H-1000 (Vector Laboratories) and observed using a Zeiss Axio Imager M2 equipped with ApoTome. 2. Specificity of the signals was established by comparison to appropriate controls.

Primary antibodies used were rabbit anti-corazonin (1:1500, obtained from Jae H. Park, University of Tennessee), mouse anti-Dachshund (clone: mAbdac2–3, 1:200, DSHB), rat anti-Deadpan (clone: 11D1BC7, 1:50, Abcam), mouse anti-Fasciclin II (clone: 1D4, 1:500, DSHB), mouse anti-P-Galactosidase (LacZ) (clone: 40–1a, 1:500, DSHB), mouse anti-GFP (clone: GFP-20, 1:1000, Sigma) and chicken anti-GFP (1:1000, Abcam). Guinea pig anti-EcI antibodies were generated against the peptide EVSESKQPITPAPDTTV and affinity-purified by Pierce Biotechnology, Inc. Secondary antibodies used were Alexa Fluor 488 goat anti-chicken (1:500, Thermo Fisher Scientific), Alexa Fluor 488 goat anti-mouse (1:500, Thermo Fisher Scientific), Alexa Fluor 488 goat anti-rabbit (1:500, Thermo Fisher Scientific), Alexa Fluor 546 goat anti-guinea pig (1:500, Thermo Fisher Scientific), Alexa Fluor 546 goat anti-mouse (1:500, Thermo Fisher Scientific), and Alexa Fluor 546 goat anti-rat (1:500, Thermo Fisher Scientific).

***Ex Vivo* CNS Culture—**Mid-third instar larvae (24 hAL3E) were surface sterilized by 70% EtOH for 1 min, rinsed in sterile PBS, and dissected in Schneider's *Drosophila* medium (Gibco). The ring gland and imaginal disks attached to the CNS were carefully removed. Dissected CNS was pre-cultured in 3 ml/well of Schneider's *Drosophila* medium containing 1% Penicillin-streptomycin solution (PSS; Thermo Fisher Scientific) in a sterile petri dish (Olympus plastics) for 30 min. After pre-incubation, tissues were transferred to the wells

containing 900 μl of Schneider's *Drosophila* medium with 1% PSS in a 24-well clear flat bottom multiwell tissue culture plate (CytoOne). Five tissues cultured per each well were dosed with 100 μl of indicated compounds in Schneider's *Drosophila* medium containing 1% PSS (total 1 ml/well) and cultured at 25°C for 16 hours *(EcRE-LacZ* reporter expression analysis) or 4 hours (EdU incorporation analysis). For *EcRE-LacZ* reporter expression analysis, cultured tissues were fixed and immunostained as described above. For EdU incorporation analysis, cultured tissues were labeled with EdU, fixed and stained as described below.

EdU Incorporation Analysis—EdU incorporation was performed using Click-iT EdU Alexa Fluor 555 Imaging Kit (Thermo Fisher Scientific). The CNS dissected from mid-third instar larvae (24 hAL3E) was cultured with EtOH (0.1 %) or 20E (1×10^{-7} M) as described above. 3 hours and 40 min after incubation with EtOH or 20E, 2 μl of 10 mM EdU was added to the 1 ml cultured medium (20 μM final concentration), and the tissues were further incubated at 25°C for 20 min (total 4 hours of incubation with EtOH or 20E). EdU-labeled tissues were fixed with 4% PFA/BBS containing 0.1% TritonX-100 for 20 min at RT, washed multiple times with PBS containing 0.3% Triton X-100 (0.3% PBST), blocked with 3% bovine serum albumin (BSA) in 0.3% PBST for 1 hour, and then incubated with Click-iT reaction cocktail including Alexa Fluor azide for 30 min. After washing multiple times with 0.3% PBST, DNA was stained with Hoechst 33342 (Thermo Fisher Scientific) at 1:2000 in 0.3% PBST with 3% BSA for 30 min at RT, and washed multiple times again with 0.3% PBST. The tissues were mounted in Vectashield H-1000 (Vector Laboratories) and observed using a Zeiss Axio Imager M2 equipped with ApoTome.2. Specificity of the signals was established by comparison to appropriate controls.

Image Analysis—For the quantification of *EcRE-LacZ* activity or EdU-positive voxels in the CNS, the total signal intensity in each brain lobe was obtained from z-stack images of the CNS and quantified using ImageJ software (NIH). The width of the stripes of medulla neuroblasts and neuroepithelium was determined by averaging measurements at three different regions in a lateral sectional image of each CNS sample by using ImageJ software. All compared images were acquired under identical parameters.

QUANTIFICATION AND STATISTICAL ANALYSIS

All statistical tests, significance levels, and sample sizes are reported in the figure legends. For the quantification of *EcRE-LacZ* activity or EdU-positive voxels in the CNS, Student's t test was used for comparison with control, whereas ANOVA with Tukey's post hoc test was used for comparison among multiple samples. Ratios of the width of the stripes of medulla neuroblasts and neuroepithelial cells from multiple samples were compared using ANOVA with Tukey's post hoc test. Prism 8 (Graphpad Software) was used for all statistical analyses.

DATA AND CODE AVAILABILITY

This study did not generate any new computer code or algorithms. Raw images used for quantitative analyses are available from the corresponding author upon request.

Supplementary Material

Refer to Web version on PubMed Central for supplementary material.

ACKNOWLEDGMENTS

We thank Vienna *Drosophila* Resource Center, Bloomington *Drosophila* Stock Center (NIH P40 OD018537), National Institute of Genetics Fly Stock Center, Kyoto Stock Center, Transgenic RNAi Project at Harvard Medical School (NIH R24 RR032668), U. Heberlein, and U. Gaul for fly stocks; J.H. Park for anti-corazonin antibody; S.H. Woodard and M.E. Adams for comments on the manuscript. The monoclonal antibodies developed by G.M. Rubin, C. Goodman, and J.R. Sanes were obtained from the Developmental Studies Hybridoma Bank, created by the Eunice Kennedy Shriver National Institute of Child Health and Human Development (NICHD) of the NIH and maintained at The University of Iowa, Department of Biology, Iowa City, IA 52242. This study was supported by a Postdoctoral Fellowship for Research Abroad from the Japan Society for the Promotion of Science to N.O., the Naito Foundation Subsidy for Dispatch of Young Researchers Abroad to N.O., an NIH Director's New Innovator Award DP2 GM132929 to N.Y., a research grant from the W.M. Keck Foundation to N.Y., and a Pew Biomedical Scholars Award from the Pew Charitable Trusts to N.Y.

REFERENCES

1. Banks WA (2012). Brain meets body: the blood-brain barrier as an endocrine interface. Endocrinology 153, 4111–4119. [PubMed: 22778219]
2. Okamoto N, Viswanatha R, Bittar R, Li Z, Haga-Yamanaka S, Perrimon N, and Yamanaka N (2018). A membrane transporter is required for steroid hormone uptake in *Drosophila*. Dev. Cell 47, 294–305. [PubMed: 30293839]
3. Yamanaka N, Rewitz KF, and O'Connor MB (2013). Ecdysone control of developmental transitions: lessons from *Drosophila* research. Annu. Rev. Entomol 58, 497–516. [PubMed: 23072462]
4. Carlson SD, Juang JL, Hilgers SL, and Garment MB (2000). Blood barriers of the insect. Annu. Rev. Entomol 45, 151–174. [PubMed: 10761574]
5. Schwabe T, Bainton RJ, Fetter RD, Heberlein U, and Gaul U (2005). GPCR signaling is required for blood-brain barrier formation in *Drosophila*. Cell 123, 133–144. [PubMed: 16213218]
6. Stork T, Engelen D, Krudewig A, Silies M, Bainton RJ, and Klämbt C (2008). Organization and function of the blood-brain barrier in *Drosophila*. J. Neurosci 28, 587–597. [PubMed: 18199760]
7. Mayer F, Mayer N, Chinn L, Pinsonneault RL, Kroetz D, and Bainton RJ (2009). Evolutionary conservation of vertebrate blood-brain barrier chemoprotective mechanisms in *Drosophila*. J. Neurosci 29, 3538–3550. [PubMed: 19295159]
8. DeSalvo MK, Mayer N, Mayer F, and Bainton RJ (2011). Physiologic and anatomic characterization of the brain surface glia barrier of *Drosophila*. Glia 59, 1322–1340. [PubMed: 21351158]
9. Limmer S, Weiler A, Volkenhoff A, Babatz F, and Klämbt C (2014). The *Drosophila* blood-brain barrier: development and function of a glial endothelium. Front. Neurosci 8, 365. [PubMed: 25452710]
10. Hindle SJ, and Bainton RJ (2014). Barrier mechanisms in the *Drosophila* blood-brain barrier. Front. Neurosci 8, 414. [PubMed: 25565944]
11. DeSalvo MK, Hindle SJ, Rusan ZM, Orng S, Eddison M, Halliwell K, and Bainton RJ (2014). The *Drosophila* surface glia transcriptome: evolutionary conserved blood-brain barrier processes. Front. Neurosci 8, 346. [PubMed: 25426014]
12. Venken KJ, Schulze KL, Haelterman NA, Pan H, He Y, Evans-Holm M, Carlson JW, Levis RW, Spradling AC, Hoskins RA, and Bellen HJ (2011). MiMIC: a highly versatile transposon insertion resource for engineering *Drosophila melanogaster* genes. Nat. Methods 8, 737–743. [PubMed: 21985007]
13. Awasaki T, Lai SL, Ito K, and Lee T (2008). Organization and postembryonic development of glial cells in the adult central brain of *Drosophila*. J. Neurosci 28, 13742–13753. [PubMed: 19091965]
14. Dominick OS, and Truman JW (1985). The physiology of wandering behaviour in *Manduca sexta.* II. The endocrine control of wandering behaviour. J. Exp. Biol 117, 45–68. [PubMed: 4067505]

15. Hall BL, and Thummel CS (1998). The RXR homolog Ultraspiracle is an essential component of the *Drosophila* ecdysone receptor. Development 125, 4709–4717. [PubMed: 9806919]
16. Davis MB, Carney GE, Robertson AE and Bender M (2005). Phenotypic analysis of *EcR-A* mutants suggests that EcR isoforms have unique functions during *Drosophila* development. Dev. Biol. 282, 385–396. [PubMed: 15950604]
17. Žitňan D, and Adams ME (2012). Neuroendocrine regulation of ecdysis In Insect Endocrinology, Gilbert LI ed. (New York, USA: Elsevier/Academic Press), pp. 253–309.
18. Koelle MR, Talbot WS, Segraves WA, Bender MT, Cherbas P, and Hogness DS (1991). The *Drosophila* EcR gene encodes an ecdysone receptor, a new member of the steroid receptor superfamily. Cell 67, 59–77. [PubMed: 1913820]
19. Sisk CL, and Foster DL (2004). The neural basis of puberty and adolescence. Nat. Neurosci 7, 1040–1047. [PubMed: 15452575]
20. McCarthy MM, and Arnold AP (2011). Reframing sexual differentiation of the brain. Nat. Neurosci 14, 677–683. [PubMed: 21613996]
21. Diotel N, Charlier TD, Lefebvre d'Hellencourt C, Couret D, Trudeau VL, Nicolau JC, Meilhac O, Kah O and Pellegrini E (2018). Steroid transport, local synthesis, and signaling within the brain: roles in neurogenesis, neuroprotection, and sexual behaviors. Front. Neurosci 12, 84. [PubMed: 29515356]
22. Truman JW (1992). Developmental neuroethology of insect metamorphosis. J. Neurobiol 23, 1404–1422. [PubMed: 1487742]
23. Truman JW (1996). Steroid receptors and nervous system metamorphosis in insects. Dev. Neurosci 18, 87–101. [PubMed: 8840088]
24. Consoulas C, Duch C, Bayline RJ, and Levine RB (2000). Behavioral transformations during metamorphosis: remodeling of neural and motor systems. Brain Res. Bull 53, 571–583. [PubMed: 11165793]
25. Veverytsa L, and Allan DW (2013). Subtype-specific neuronal remodeling during *Drosophila* metamorphosis. Fly (Austin) 7, 78–86. [PubMed: 23579264]
26. Boulanger A, and Dura JM (2015). Nuclear receptors and *Drosophila* neuronal remodeling. Biochim. Biophys. Acta 1849, 187–195. [PubMed: 24882358]
27. Yaniv SP, and Schuldiner O (2016). A fly's view of neuronal remodeling. Wiley Interdiscip. Rev. Dev. Biol 5, 618–635. [PubMed: 27351747]
28. Syed MH, Mark B, and Doe CQ (2017). Playing well with others: extrinsic cues regulate neural progenitor temporal identity to generate neuronal diversity. Trends Genet. 33, 933–942. [PubMed: 28899597]
29. Lanet E, Gould AP, and Maurange C (2013). Protection of neuronal diversity at the expense of neuronal numbers during nutrient restriction in the *Drosophila* visual system. Cell Rep. 3, 587–594. [PubMed: 23478023]
30. Yasugi T, Umetsu D, Murakami S, Sato M, and Tabata T (2008). *Drosophila* optic lobe neuroblasts triggered by a wave of proneural gene expression that is negatively regulated by JAK/STAT. Development 135, 1471–1480. [PubMed: 18339672]
31. Lee T, Marticke S, Sung C, Robinow S, and Luo L (2000). Cell-autonomous requirement of the USP/EcR-B ecdysone receptor for mushroom body neuronal remodeling in *Drosophila*. Neuron 28, 807–818. [PubMed: 11163268]
32. Awasaki T, and Lee T (2011). Orphan nuclear receptors control neuronal remodeling during fly metamorphosis. Nat. Neurosci 14, 6–7. [PubMed: 21187848]
33. Choi YJ, Lee G, and Park JH (2006). Programmed cell death mechanisms of identifiable peptidergic neurons in *Drosophila melanogaster*. Development 133, 2223–2232. [PubMed: 16672345]
34. Yamanaka N, Marqués G, and O'Connor MB (2015). Vesicle-mediated steroid hormone secretion in *Drosophila melanogaster*. Cell 163, 907–919. [PubMed: 26544939]
35. Champlin DT, and Truman JW (1998). Ecdysteroid control of cell proliferation during optic lobe neurogenesis in the moth *Manduca sexta*. Development 125, 269–277. [PubMed: 9486800]
36. Minakuchi C, Nakagawa Y, Kamimura M, and Miyagawa H (2005). Measurement of receptor-binding activity of non-steroidal ecdysone agonists using in vitro expressed receptor proteins

(EcR/USP complex) of Chilo suppressalis and Drosophila melanogaster In New Discoveries in Agrochemicals, Clark JM, and Ohkawa H, eds. (Washington DC, USA: American Chemical Society), pp. 191–200.

37. Abbott NJ, Ronnback L, and Hansson E (2006). Astrocyte-endothelial interactions at the blood-brain barrier. Nat. Rev. Neurosci 7, 41–53. [PubMed: 16371949]
38. Saunders NR, Liddelow SA, and Dziegielewska KM (2012). Barrier mechanisms in the developing brain. Front Pharmacol 3, 46. [PubMed: 22479246]
39. Obermeier B, Daneman R, and Ransohoff RM (2013). Development, maintenance and disruption of the blood-brain barrier. Nat. Med 19, 1584–1596. [PubMed: 24309662]
40. Uhr M, Holsboer F, and Muller MB (2002). Penetration of endogenous steroid hormones corticosterone, cortisol, aldosterone and progesterone into the brain is enhanced in mice deficient for both mdrla and mdrlb P-glycoproteins. J. Neuroendocrinol 14, 753–759. [PubMed: 12213137]
41. Hindle SJ, Munji RN, Dolghih E, Gaskins G, Orng S, Ishimoto H, Soung A, DeSalvo M, Kitamoto T, Keiser MJ, et al. (2017). Evolutionarily conserved roles for blood-brain barrier xenobiotic transporters in endogenous steroid partitioning and behavior. Cell Rep. 21, 1304–1316. [PubMed: 29091768]
42. Pardridge WM (2007). Blood-brain barrier delivery. Drug Discov. Today 12, 54–61. [PubMed: 17198973]
43. Ayloo S, and Gu C (2019). Transcytosis at blood-brain barrier. Curr. Opin. Neurobiol 57, 32–38. [PubMed: 30708291]
44. Ohtsuki S, and Terasaki T (2007). Contribution of carrier-mediated transport systems to the blood-brain barrier as a supporting and protecting interface for the brain; importance for CNS drug discovery and development. Pharm. Res 24, 1745–1758. [PubMed: 17619998]
45. Truman JW, Talbot WS, Fahrbach SE, and Hogness DS (1994). Ecdysone receptor expression in the CNS correlates with stage-specific responses to ecdysteroids during *Drosophila* and *Manduca* development. Development 120, 219–234. [PubMed: 8119129]
46. Hennemann G, Docter R, Friesema EC, de Jong M, Krenning EP, and Visser TJ (2001). Plasma membrane transport of thyroid hormones and its role in thyroid hormone metabolism and bioavailability. Endocr. Rev 22, 451–476. [PubMed: 11493579]
47. Abe T, Suzuki T, Unno M, Tokui T, and Ito S (2002). Thyroid hormone transporters: recent advances. Trends Endocrinol. Metab 13, 215–20. [PubMed: 12185668]
48. Visser WE, Friesema EC, and Visser TJ (2011). Minireview: thyroid hormone transporters: the knowns and the unknowns. Mol. Endocrinol 25, 1–14. [PubMed: 20660303]
49. Bernal J, Guadano-Ferraz A, and Morte B (2015). Thyroid hormone transporters-functions and clinical implications. Nat. Rev. Endocrinol 11, 406–417. [PubMed: 25942657]
50. Braun D, and Schweizer U (2018). Thyroid hormone transport and transporters. Vitam. Horm 106, 19–44. [PubMed: 29407435]
51. Hagenbuch B (2007). Cellular entry of thyroid hormones by organic anion transporting polypeptides. Best Pract. Res. Clin. Endocrinol. Metab 21, 209–221. [PubMed: 17574004]
52. Wirth EK, Schweizer U, and Kohrle J (2014). Transport of thyroid hormone in brain. Front. Endocrinol 5, 98.
53. Landers K, and Richard K (2017). Traversing barriers - how thyroid hormones pass placental, blood-brain and blood-cerebrospinal fluid barriers. Mol. Cell. Endocrinol 458, 22–28. [PubMed: 28153799]
54. Bernal J (2018). New insights on thyroid hormone and the brain. Curr. Opin. Endocr. Metab. Res 2, 24–28.
55. Dumitrescu AM, Liao X-H, Best TB, Brockmann K, and Refetoff S (2004). A novel syndrome combining thyroid and neurological abnormalities is associated with mutations in a monocarboxylate transporter gene. Am. J. Hum. Genet 74, 168–175. [PubMed: 14661163]
56. Friesema ECH, Grueters A, Biebermann H, Krude H, von Moers A, Reeser M, Barrett TG, Mancilla EE, Svensson J, Kester MHA, et al. (2004). Association between mutations in a thyroid hormone transporter and severe X-linked psychomotor retardation. Lancet 364, 1435–1437. [PubMed: 15488219]

57. Vatine GD, Al-Ahmad A, Barriga BK, Svendsen S, Salim A, Garcia L, Garcia VJ, Ho R, Yucer N, Qian T, et al. (2017). Modeling psychomotor retardation using iPSCs from MCT8-defcient patients indicates a prominent role for the blood-brain barrier. Cell Stem Cell 20, 831–843. [PubMed: 28526555]

58. Strømme P, Groeneweg S, Lima de Souza EC, Zevenbergen C, Torgersbråten A, Holmgren A, Gurcan E, Meima ME, Peeters RP, Visser WE, et al. (2018). Mutated thyroid hormone transporter OATP1C1 associates with severe brain hypometabolism and juvenile neurodegeneration. Thyroid 28, 1406–1415. [PubMed: 30296914]

59. Kalliokoski A, and Niemi M (2009). Impact of OATP transporters on pharmacokinetics. Br. J. Pharmacol 158, 693–705. [PubMed: 19785645]

HIGHLIGHTS

- Insect steroid hormone ecdysone cannot freely diffuse across the blood-brain barrier
- Ecdysone requires an SLCO superfamily transporter EcI in the BBB to enter the brain
- *EcI* knockdown in the BBB blocks ecdysone-mediated neuronal events during development
- Steroid hormone permeability across the BBB may affect brain development and behavior

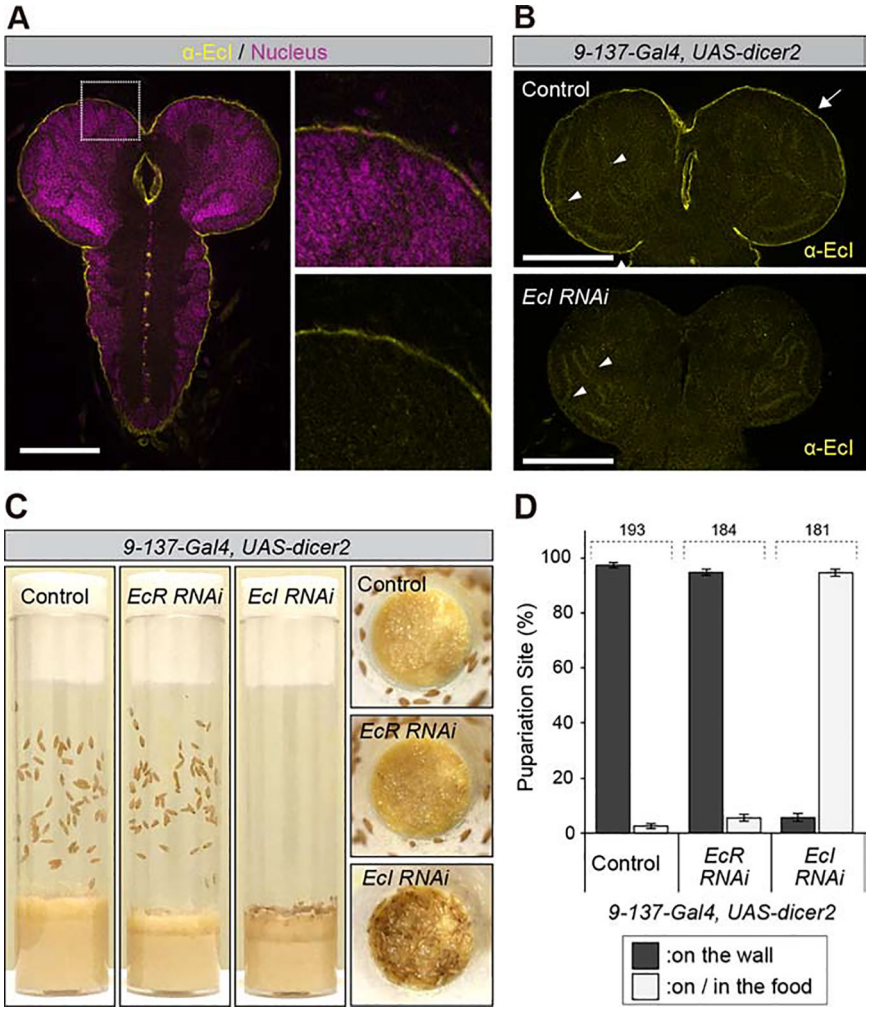

Figure 1. EcI Is Highly Expressed in the BBB and Required for Normal Wandering Behavior.

(A) EcI immunoreactivity (yellow) in the CNS of control (w^{1118}) L3 larvae. Nuclei were stained with Hoechst 33342 (magenta). Enlarged images correspond to the boxed area. Scale bar, 100 μm.

(B) EcI immunoreactivity (yellow) in the CNS of control and *EcI* RNAi L3 larvae. *9–137-Gal4 > UAS-dicer2* was used to induce RNAi in the BBB. White arrows indicate EcI immunoreactivity in the BBB. White arrowheads indicate EcI immunoreactivity in neuroepithelial cells of the inner and outer proliferation centers. Cross-section images are shown. Scale bars, 100 μm.

(C) Representative images of culture vials of control, *EcR* RNAi, and *EcI* RNAi animals after puparium formation. Right images correspond to the images of the surface of the food in each vial.

(D) Percentages of animals pupariated on the vial wall (dark gray) or on/in the food (light gray). All values are the means ± SD of four independent experiments. Numbers of animals observed are shown on top of each genotype.

See also Figures S1 and S2 for related results.

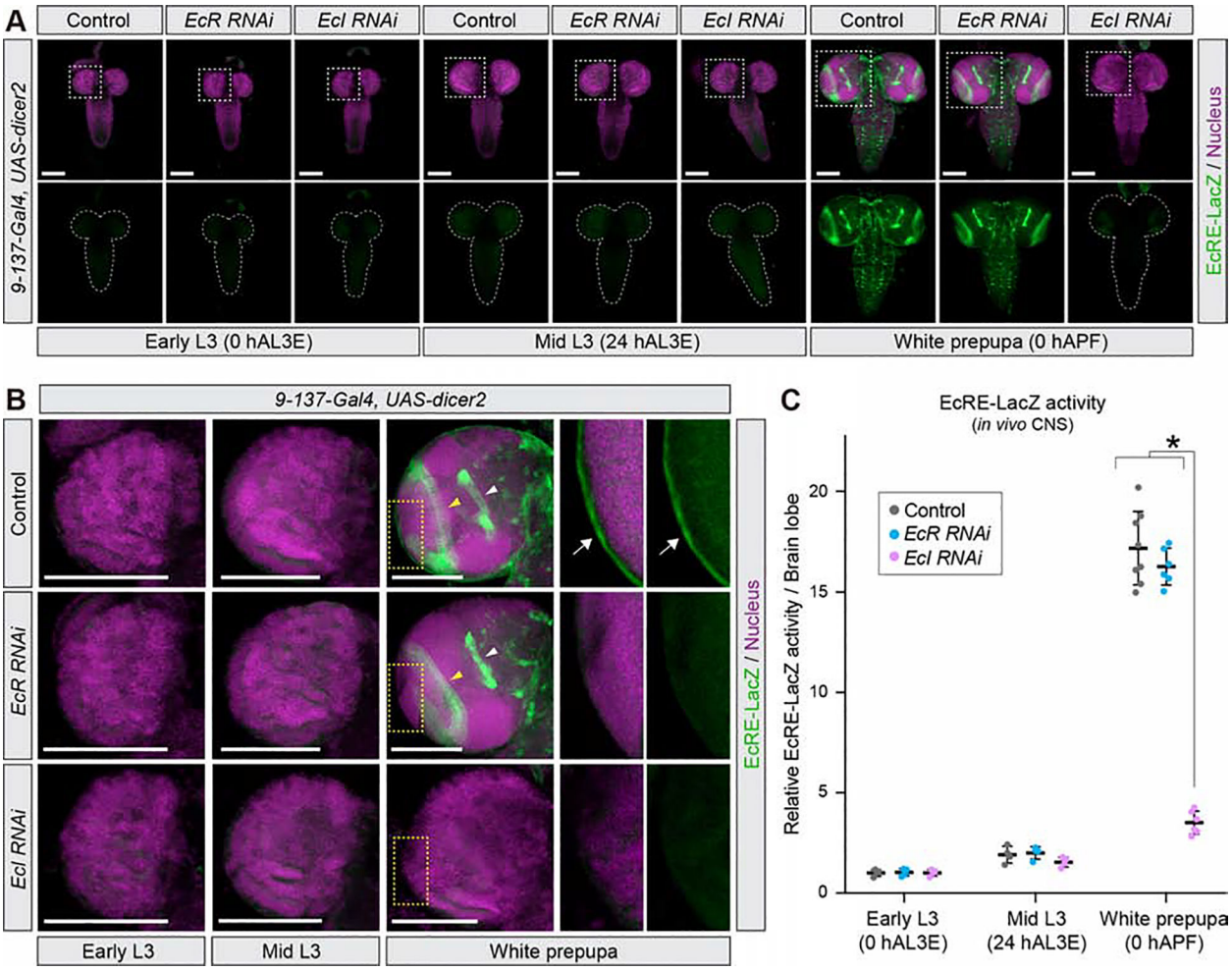

Figure 2. EcI but not EcR in the BBB Is Required for the Activation of Ecdysone Signaling within the CNS.

(A) *EcRE-LacZ* reporter activity (green) in the CNS of control, *EcR* RNAi, and *EcI* RNAi animals at early L3 (0 hour after L3 ecdysis [0 hAL3E]), mid L3 (24 hAL3E), and white prepupal (0 hour after puparium formation [0 hAPF]) stages. *9–137-Gal4 > UAS-dicer2* was used to induce RNAi in the BBB. Nuclei were stained with Hoechst 33342 (magenta). Scale bars, 100 μm.

(B) Enlarged images that correspond to the boxed areas in (A). White and yellow arrowheads indicate *EcRE-LacZ* expression in the inner and outer proliferation centers, respectively; Enlarged images correspond to the cross-section images of the yellow boxed area. White arrows indicate *EcRE-LacZ* expression in the BBB. WP, white prepupa. Scale bars, 100 μm.

(C) Relative *EcRE-LacZ* expression quantified by the LacZ signal intensity in each brain lobe. Values are shown as fold changes relative to the control level (0 hAL3E). All values are the means ± SD (n = 4–8). *p < 0.0001 from ANOVA with Tukey's post hoc test compared to control or *EcR* RNAi.

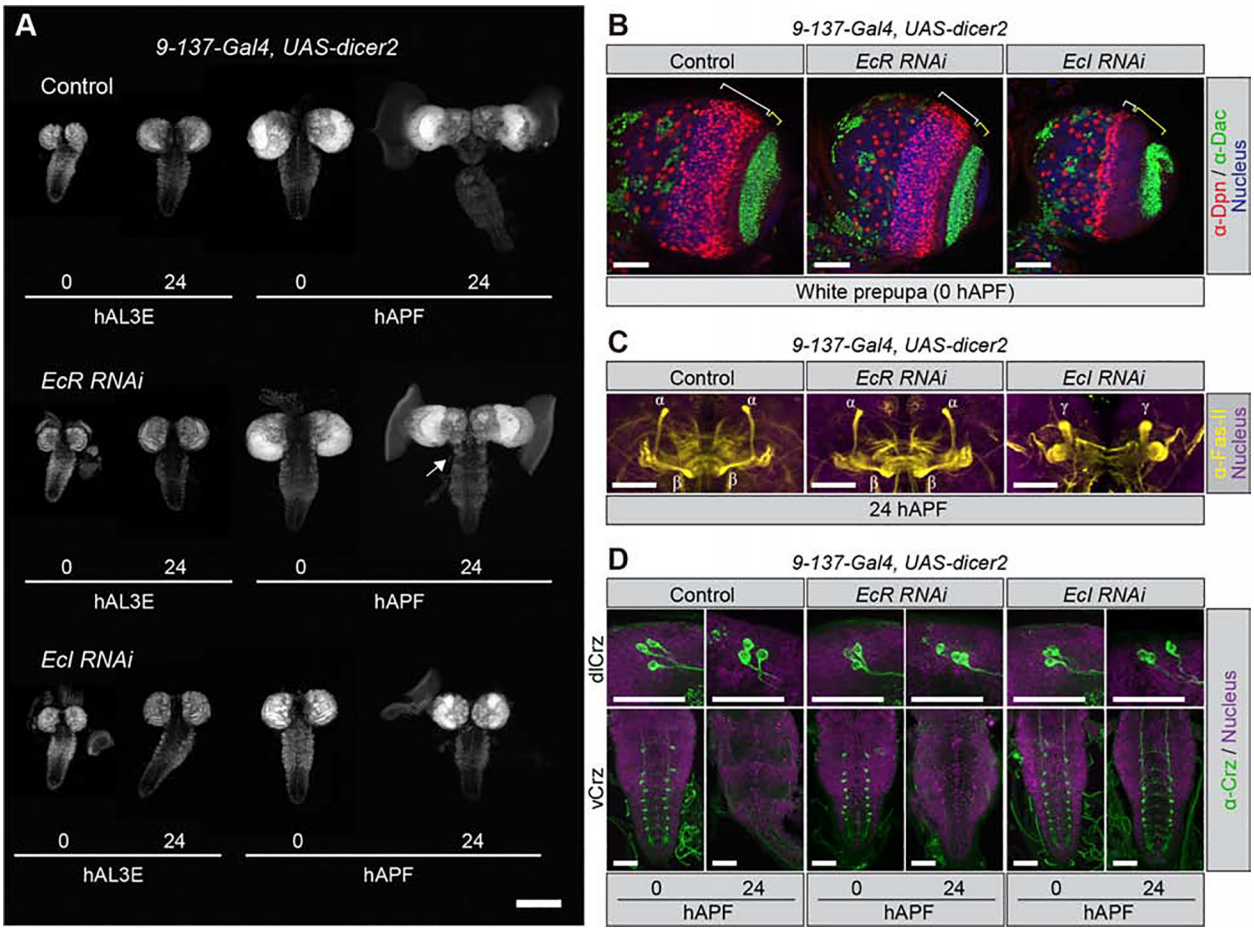

Figure 3. EcI in the BBB Is Required for Ecdysone-Mediated Neuronal Events during Development.

(A) Developmental changes of the CNS morphology in control, *EcR* RNAi, and *EcI* RNAi animals. *9–137-Gal4 > UAS-dicer2* was used to induce RNAi in the BBB. Nuclei in the CNS were stained with Hoechst 33342. Representative images of the CNS at different stages were combined into a single panel. White arrow indicates the failure of the separation of the subesophageal and thoracic ganglia in the CNS of *EcR* RNAi animals. Consistent phenotypes were observed in all samples examined (n = 10–20 CNS samples per genotype). Scale bar, 200 μm.

(B, C, D) Ecdysone-mediated neuronal differentiation (B), remodeling (C) and apoptosis (D) during development. *9–137-Gal4 > UAS-dicer2* was used to induce RNAi in the BBB. Nuclei were stained with Hoechst 33342. Scale bars, 50 μm. (B) CNS Immunostaining at 0 hAPF for Deadpan (Dpn) and Dachshund (Dac) to label neuroblasts and lamina neurons, respectively. Lateral views of the brain optic lobe are shown. Regions of medulla neuroblasts and neuroepithelial cells were determined according to [30] and indicated by white and yellow brackets, respectively. (C) CNS Immunostaining at 24 hAPF for Fasciclin-II (Fas-II) to label mushroom body lobes. α and β indicate newly extending axonal lobes of α/β neurons, and γ indicates larval-specific axonal lobe of γ neurons. Consistent phenotypes were observed in all samples examined (n = 18–22 CNS samples per genotype). (D) CNS Immunostaining at 0 and 24 hAPF for corazonin. Upper panels show dorso-lateral

corazonin-producing neurons (dlCrz) and lower panels show ventral nerve cord corazonin-producing neurons (vCrz).

See also Figure S3 for quantitative analyses of (B) and (D).

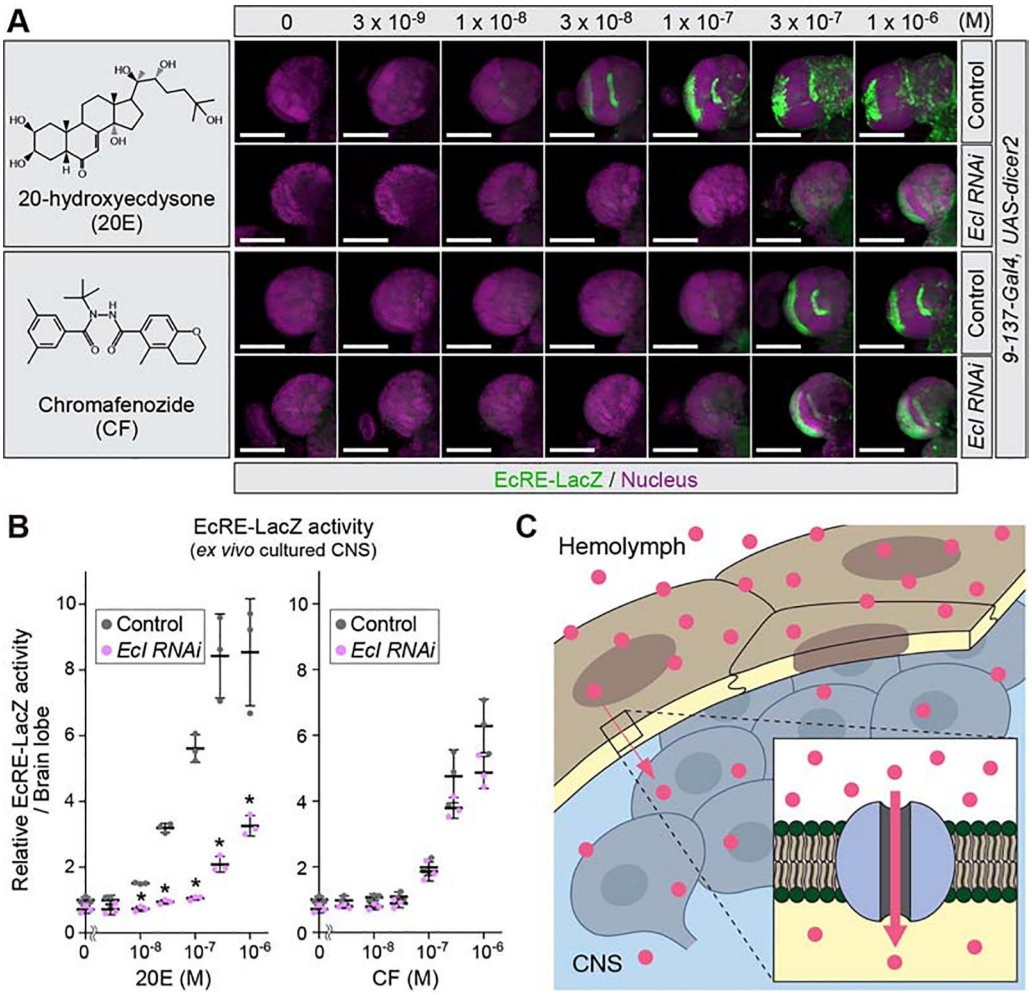

Figure 4. EcI in the BBB Is Required for Ecdysone Incorporation from Circulation into the CNS.

(A) *EcRE-LacZ* reporter activity (green) in the CNS from control and *EcI* RNAi animals at mid-L3 (24 hAL3E) larvae cultured *ex vivo* for 16 hours with various concentrations of 20-hydroxyecdysone (20E) or chromafenozide (CF). *9–137-Gal4 > UAS-dicer2* was used to induce RNAi in the BBB. Nuclei were stained with Hoechst 33342 (magenta).

(B) Relative *EcRE-LacZ* expression levels quantified by the LacZ signal intensity in each brain lobe. Values are shown as fold changes relative to the control level (0 M). All values are the means ± SD (n = 3). *p < 0.01 from Student's t test compared to control. Scale bars, 100 μm.

(C) Schematic model of EcI-mediated incorporation of ecdysone (pink circles) across the BBB.

See also Figure S4 for related results.

KEY RESOURCES TABLE

REAGENT or RESOURCE	SOURCE	IDENTIFIER
Antibodies		
Chicken anti-GFP	Abcam	Cat#: ab13970; RRID: AB_300798
Goat anti-Chicken IgY, Alexa Fluor 488	Thermo Fisher Scientific	Cat#: A-11039; RRID: AB_2534096
Goat anti-Guinea pig IgG, Alexa Fluor 546	Thermo Fisher Scientific	Cat#: A-11074; RRID: AB_2534118
Goat anti-Mouse IgG, Alexa Fluor 488	Thermo Fisher Scientific	Cat#: A-11029; RRID: AB_2534088
Goat anti-Mouse IgG, Alexa Fluor 546	Thermo Fisher Scientific	Cat#: A-11030; RRID: AB_2534089
Goat anti-Rabbit IgG, Alexa Fluor 488	Thermo Fisher Scientific	Cat#: A-11034; RRID: AB_2576217
Goat anti-Rat IgG, Alexa Fluor 546	Thermo Fisher Scientific	Cat#: A-11081; RRID: AB_2534125
Guinea pig anti-EcI	This paper	N/A
Mouse anti-Dachshund (clone: mAbdac2–3)	DSHB	Cat#: mAbdac2–3; RRID: AB_528190
Mouse anti-Fasciclin II (clone: 1D4)	DSHB	Cat#: 1D4 anti-Fasciclin II; RRID: AB_528235
Mouse anti-β-Galactosidase (LacZ) (clone: 40–1a)	DSHB	Cat#: 40–1a; RRID: AB_528100
Mouse anti-GFP (clone: GFP-20)	Sigma	Cat#: G6539; RRID: AB_259941
Rabbit anti-Corazonin	Obtained from Jae H. Park (University of Tennessee)	N/A
Rat anti-Deadpan (clone: 11D1BC7)	Abcam	Cat#: ab195173; RRID: AB_2687586
Chemicals, Peptides, and Recombinant Proteins		
8% Paraformaldehyde Aqueous Solution	Electron Microscopy Sciences	Cat#: 157–8
20-Hydroxyecdysone	Sigma-Aldrich	Cat#: H5142–10MG
Chromafenozide	Sigma-Aldrich	Cat#: 32352–50MG
Ethanol	Decon	Cat#: 2716
Hoechst 33342	Thermo Fisher Scientific	Cat#: H3570
Critical Commercial Assays		
Click-iT EdU Alexa Fluor 555 Imaging Kit	Thermo Fisher Scientific	Cat#: C10338
Experimental Models: Organisms/Strains		
D. melanogaster: *9–137-Gal4*	Obtained from Ulrike Heberlein (Janelia Research Campus)	N/A
D. melanogaster: *EcRE-LacZ*	Bloomington Drosophila Stock Center	BDSC: 4516
D. melanogaster: *EcRE-LacZ*	Bloomington Drosophila Stock Center	BDSC: 4517
D. melanogaster: *Mi{MIC}Oatp74D* ^{MI05878} (*EcI* ^{MI05878})	Bloomington Drosophila Stock Center	BDSC: 42353
D. melanogaster: *Moody-Gal4*	Obtained from Ulrike Gaul (Ludwig-Maximilians-Universität München)	N/A
D. melanogaster: *NP2276-Gal4*	Kyoto Drosophila Genomics and Genetic Resources	Kyoto DGGR: 112853
D. melanogaster: *NP6293-Gal4*	Kyoto Drosophila Genomics and Genetic Resources	Kyoto DGGR: 105188
D. melanogaster: *UAS-dicer2*	Vienna Drosophila Resource Center	VDRC: 60008
D. melanogaster: *UAS-dicer2*	Vienna Drosophila Resource Center	VDRC: 60009
D. melanogaster: *UAS-EcI (Oatp74D) RNAi*	National Institute of Genetics	NIG: 7571R-1

REAGENT or RESOURCE	SOURCE	IDENTIFIER
D. melanogaster: *UAS-EcR RNAi*	Bloomington Drosophila Stock Center	BDSC: 9327
D. melanogaster: *UAS-mCD8-GFP*	Bloomington Drosophila Stock Center	BDSC: 5130
D. melanogaster: w^{1118}	Bloomington Drosophila Stock Center	BDSC: 5905
Software and Algorithms		
ImageJ 1.48v	NIH	https://imagej.nih.gov/ij/
Prism 8	Graphpad Software Inc.	www.graphpad.com